


 Cite this: *Chem. Commun.*, 2024, 60, 10544

 Received 29th June 2024,  
 Accepted 29th August 2024

DOI: 10.1039/d4cc03101f

rsc.li/chemcomm

# Investigating the radical properties of oxidized carbon materials under photo-irradiation: behavior of carbon radicals and their application in catalytic reactions†

 Md Razu Ahmed,<sup>ab</sup> Israel Ortiz Anaya<sup>a</sup> and Yuta Nishina<sup>ab\*</sup>

Oxidized carbon materials have abundant surface functional groups and customizable properties, making them an excellent platform for generating radicals. Unlike reactive oxygen species such as hydroxide or superoxide radicals that have been reported previously, oxidized carbon also produces stable carbon radicals under photo-irradiation. This has been confirmed through electron spin resonance. Among the various oxidized carbon materials synthesized, graphene oxide shows the largest number of carbon radicals when exposed to blue LED light. The light absorption capacity, high surface area, and unique structural characteristics of oxidized carbon materials offer a unique function for radical-mediated oxidative reactions.

Free radicals play a crucial role in many fields such as catalysis, chemical synthesis, biomedicine, and antioxidants in personal care products.<sup>1–3</sup> Various free radicals used in many industries are toxic and explosive, and due to the coupling of individual radicals, they lack sufficient stability for long-term storage.<sup>4,5</sup> Developing stable, low-cost, and environmentally friendly radicals remains challenging. Carbon-based materials have received growing interest due to their unique properties, such as high surface area, electron conductivity, biocompatibility, environmental sustainability, and versatility.<sup>6,7</sup> Carbon materials can generate free radicals under thermal treatment<sup>8–10</sup> and photo-irradiation.<sup>11,12</sup> However, in the thermal process, carbon materials are concurrently decomposed, and radicals rapidly disappear.<sup>13,14</sup> Conversely, in the photo-irradiation process, carbon materials are mildly activated to produce free radicals.<sup>15–18</sup> Electrons tend to localize at the edge or defect sites of the carbon plane, which enhances their reactivity and stability as free radicals.<sup>19–22</sup> In this study, we produce various oxidized carbon materials and investigate their properties for generating carbon radicals under visible light irradiation. The resulting radical species are utilized for catalysis in

the oxidative dehydrogenation of indoline and the oxidative coupling of benzylamine.

Various carbon materials such as graphite, activated carbon (AC), carbon black (CB), carbon nanotube (CNT), and nanodiamond (ND) were oxidized. After oxidation, oxidized carbon materials were described as follows: graphene oxide (GO) from graphite, oxidized activated carbon (O-AC) from AC, oxidized carbon black (O-CB) from CB, oxidized carbon nanotube (O-CNT) from CNT, oxidized nanodiamond (O-ND) from ND.

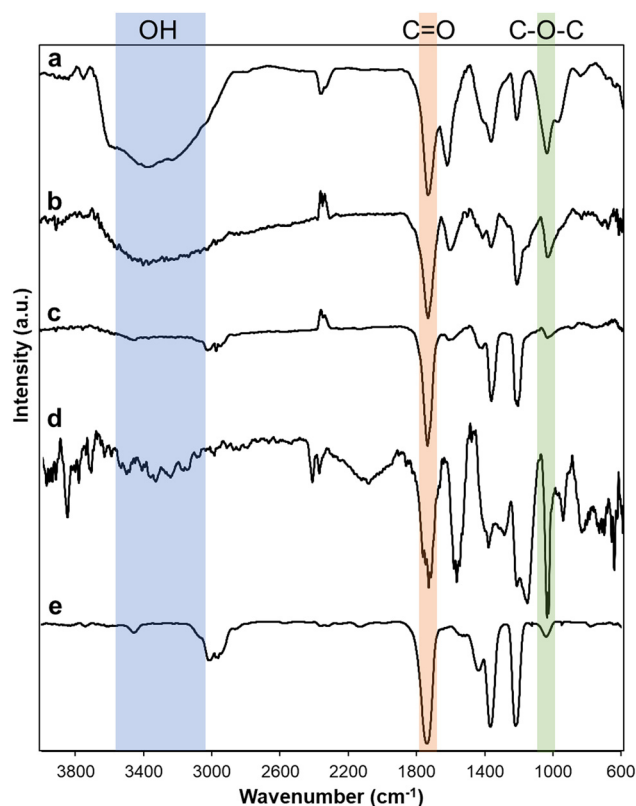


Fig. 1 FTIR spectra of (a) GO, (b) O-AC, (c) O-CB, (d) O-CNT, and (e) O-ND.

<sup>a</sup> Research Institute for Interdisciplinary Science, Okayama University, 3-1-1 Tsushimanaka, Kita-ku, Okayama 700-8530, Japan  
 E-mail: nisina-y@cc.okayama-u.ac.jp

<sup>b</sup> Faculty of Science, Bangabandhu Sheikh Mujibur Rahman Science and Technology University, Gopalganj 8100, Bangladesh

† Electronic supplementary information (ESI) available. See DOI: <https://doi.org/10.1039/d4cc03101f>



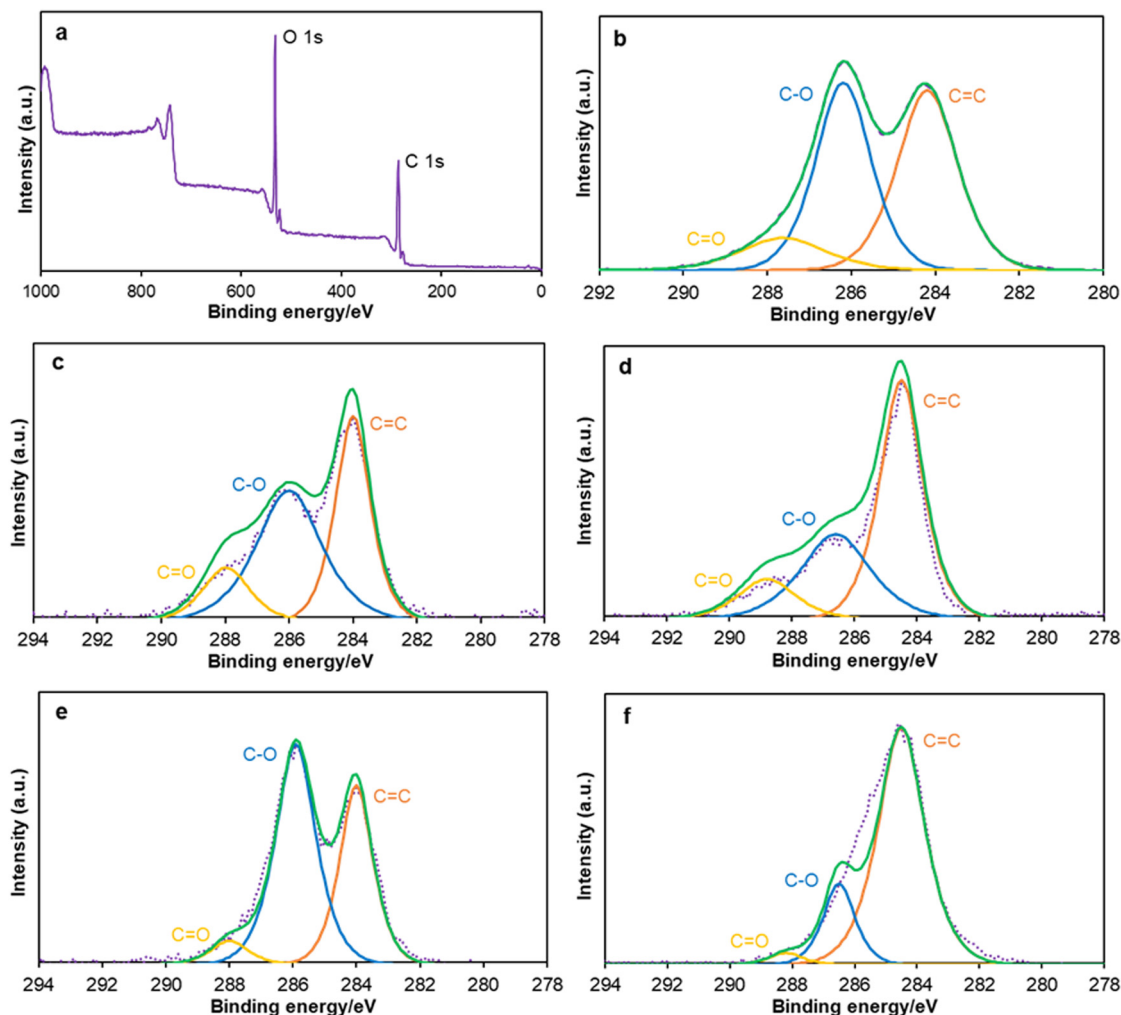


Fig. 2 XPS (a) survey spectra of GO, (b) C 1s region of GO, (c) C 1s region of O-AC, (d) C 1s region of O-CB, (e) C 1s region of O-CNT, and (f) C 1s region of O-ND.

Oxidized carbon materials were characterized by Fourier transform infrared (FTIR) and X-ray photoelectron spectroscopy (XPS). A broad peak of FTIR spectra ranging from  $3600\text{ cm}^{-1}$  to  $2600\text{ cm}^{-1}$  indicates the presence of hydroxyl groups (Fig. 1). Characteristic peaks centered at  $1735\text{ cm}^{-1}$  and  $1030\text{ cm}^{-1}$  are carbonyl and epoxide groups, respectively. FTIR spectra showed that GO, O-AC, O-CB, and O-CNT have hydroxyl, carbonyl, and epoxide functional groups, but O-ND contains only carbonyl and epoxide groups (Fig. 1e). In all oxidized carbon materials, the intensity of carbonyl group peaks was significant. In the case of GO (Fig. 1a) and O-CNT (Fig. 1d), the intensity of the epoxide peaks is higher than other oxidized carbon materials, probably because graphite and CNT have large  $\text{sp}^2$  domains.

All XPS survey spectra showed a similar pattern; a typical example of GO is shown in Fig. 2a, and others are listed in the ESI† (Fig. S6–S9). XPS survey spectra indicate that GO has more oxygen-containing groups than other oxidized carbons (Fig. 2a). High-resolution XPS represents the C=C bonds at  $284.2\text{ eV}$ , C–O bonds at  $286.2\text{ eV}$ , and C=O bonds at  $287.8\text{ eV}$ . XPS spectra at the C 1s region of GO show a larger number of C–O

bonds than C=C bonds and C=O bonds (Fig. 2b). O-AC has a lower quantity of C–O bonds than GO (Fig. 2c) but higher than that of O-CB (Fig. 2d). Moreover, O-CNT (Fig. 2e) contains a greater number of C–O bonds than C=C bonds like GO. O-ND (Fig. 2f) has a lower number of C–O and C=O bonds than all other oxidized carbon materials.

To elucidate the photo-radical properties, *in situ* electron spin resonance (ESR) experiments were designed in the absence and presence of blue LED light irradiation (Fig. 3a and b). A mixture of oxidized carbon materials in acetonitrile was irradiated and subjected to ESR analysis. For all oxidized carbon materials, a negligible ESR signal appeared in the absence of light (Fig. 3a), in contrast, a strong ESR signal was observed by the irradiation of blue LED light (Fig. 3b). Among oxidized carbons, GO showed the highest ESR peak intensity, suggesting that more carbon radicals are generated from GO than other oxidized carbon materials under the irradiation of blue LED light.

It has been reported that epoxide can be selectively photo-excited under light irradiation, resulting in the reversible



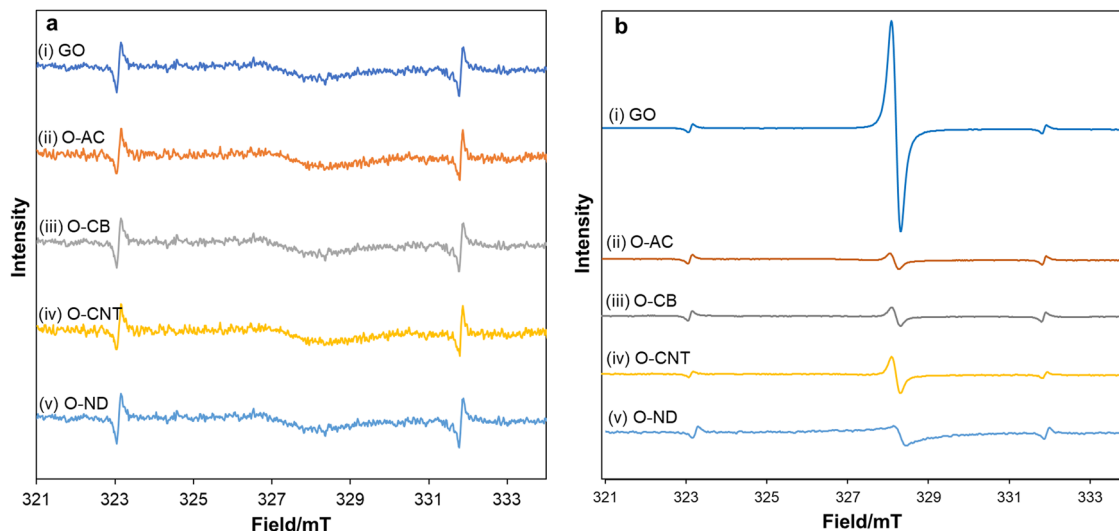
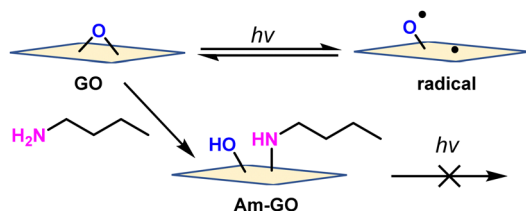
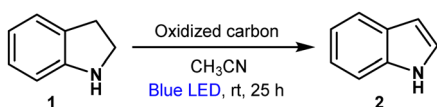


Fig. 3 ESR spectra of (i) GO, (ii) O-AC, (iii) O-CB, (iv) O-CNT, and (v) O-ND. (a) in the absence of light, and (b) under irradiation of blue LED light. The standard  $\text{Mn}^{2+}$  peaks are observed at 323 and 332 mT.



Scheme 1 Mechanistic route of generating radicals from GO and Am-GO under light irradiation (for simplicity, only the epoxide functional group is shown).

Table 1 Evaluation of the catalytic activity of oxidized carbon materials by oxidation of indoline<sup>a</sup>

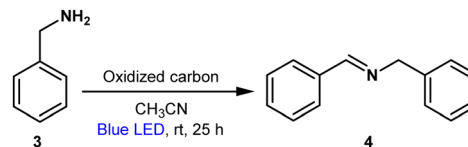


Entry	Oxidized carbon	Yield <sup>b</sup> (%)
1	GO	85
2	O-AC	12
3	O-CB	10
4	O-CNT	7
5	O-ND	5
6 <sup>c</sup>	GO	0
7	—	0
8 <sup>d</sup>	GO	85
9 <sup>e</sup>	GO	84

<sup>a</sup> Reaction conditions: indoline **1** (0.2 mmol), oxidized carbon (5 mg),  $\text{CH}_3\text{CN}$  (1.0 mL) under air atmosphere at room temperature, irradiation of blue LED for 25 h. <sup>b</sup> GC yield. <sup>c</sup> Without photo-irradiation. <sup>d</sup> Under Ar. <sup>e</sup>  $\text{O}_2$ -saturated  $\text{CH}_3\text{CN}$  was used.

generation of carbon radicals.<sup>23,24</sup> GO contains a greater number of epoxides, as evidenced by FTIR and XPS analysis, which

Table 2 Evaluation of the catalytic activity of oxidized carbon materials by oxidative coupling of benzylamine<sup>a</sup>



Entry	Oxidized carbon	Yield <sup>b</sup> (%)
1	GO	90
2	O-AC	10
3	O-CB	5
4	O-CNT	7
5	O-ND	3
6 <sup>c</sup>	GO	0
7	—	0
8 <sup>d</sup>	GO	90
9 <sup>e</sup>	GO	90

<sup>a</sup> The reaction conditions: benzylamine **3** (0.2 mmol), oxidized carbon (5 mg),  $\text{CH}_3\text{CN}$  (1.0 mL) under air atmosphere at room temperature, irradiation of blue LED for 25 h. <sup>b</sup> GC yield. <sup>c</sup> Without photo-irradiation. <sup>d</sup> Under Ar. <sup>e</sup>  $\text{O}_2$ -saturated  $\text{CH}_3\text{CN}$  was used.

explains why GO generates more carbon radicals under the irradiation of blue LED light. Regarding the stability of carbon radicals, it is intriguing that GO showed stable ESR spectra for over 6 months (Fig. S10, ESI<sup>†</sup>).

To confirm that the carbon radicals are derived from epoxide, epoxide on GO was reacted with amine. The amine-functionalized GO (Am-GO) was synthesized by following the reported literature.<sup>25,26</sup> GO and Am-GO were irradiated under blue LED light and measured ESR. As a result, GO gave a significant ESR signal (Fig. S12a, ESI<sup>†</sup>), however, an insignificant ESR signal appeared for Am-GO (Fig. S12b, ESI<sup>†</sup>). This evidence proved that the epoxide bond opens under irradiation of light and gives radical species (Scheme 1).

It has been reported that carbon radicals function as catalysts; activation of  $\text{O}_2$  to generate reactive oxygen species for



oxidation of various substrates has been well studied.<sup>27–29</sup> We have also reported the oxidation of indoline by photo-irradiation of GO.<sup>24</sup> In this research, the catalytic activity of oxidized carbon materials was evaluated by oxidation of indoline and oxidative coupling of benzylamine under irradiation of blue LED light. Using these reactions as models, we investigated the photocatalytic oxidation reactions of each oxidized carbon material. Table 1 shows the results of the oxidation reaction of indoline (1) to indole (2). From all oxidized carbon materials, GO showed a highest yield of 85% (Table 1, entry 1); however, other oxidized carbon materials such as O-AC, O-CB, O-CNT, and O-ND gave lower yields of 12%, 10%, 7%, and 5%, respectively (Table 1, entries 2–5). No desired product was observed when the reaction was conducted in the darkness and in the absence of oxidized carbon (Table 1, entries 6 and 7). The reaction also proceeded under Ar atmosphere (Table 1, entry 8), suggesting the dehydrogenative oxidation as reported previously.<sup>24</sup>

Table 2 shows the results of the oxidative coupling reaction of benzylamine (3) to imine (4). Of all oxidized carbon materials, GO showed a highest yield of 90% (Table 2, entry 1); however, other oxidized carbon materials gave lower yields (Table 2, entries 2–5). Both light and oxidized carbon were proved to be essential for this reaction; no desired product was observed when the reaction was conducted in the darkness and the absence of oxidized carbon (Table 2, entries 6–7). The reaction also proceeded under Ar atmosphere (Table 2, entry 8).

All oxidized carbon materials showed the presence of carbon radicals under irradiation of blue LED light as shown in Fig. 3b. Among them, GO radical peak intensity was the highest and gave the highest yield for oxidation of indoline and oxidative coupling of benzylamine. The radical peak intensity of O-AC, O-CB, O-CNT, and O-ND were lower and yielded lower for the oxidation product. Moreover, both of the reactions also proceeded under Ar atmosphere, suggesting dehydrogenative reactions and carbon radicals were responsible for the proceeding of these reactions.

In conclusion, the distinctive properties of oxidized carbon materials result from their unique structure, functional groups, and chemical reactivity, which enable them to produce radicals. The quantity of radicals varies among different types of oxidized carbons; GO exhibited the largest number of radicals when exposed to blue LED light. When GO is photoexcited by blue LED light, it promotes the oxidation of indoline and benzylamine. These properties make oxidized carbon materials versatile for potential applications in catalysis, as well as environmental remediation, energy storage, and biomedical engineering.

M. R. A. was supported by the MEXT scholarship. Y. N. was supported by JST CREST (Grant No. JPMJCR18R3) and JSPS KAKENHI (23H01101, 23K25798).

## Data availability

The data supporting this article have been included as part of the ESI.†

## Conflicts of interest

There are no conflicts to declare.

## Notes and references

- P. Eskandari, Z. A. Rezvani, H. R. Mamaqani and M. S. Kalajahi, *Adv. Colloid Interface Sci.*, 2021, **294**, 102471.
- A. Phaniendra, D. B. Jestadi and L. Periyasamy, *Ind. J. Clin. Biochem.*, 2015, **30**, 11.
- C. Kingston, R. Zepp, A. Andrad, D. Boverhof, R. Fehir, D. Hawkins, J. Roberts, P. Sayre, B. Shelton, Y. Sultan, V. Vejins and W. Wohlleben, *Carbon*, 2014, **68**, 33.
- M. Chen, M. Zhong and J. A. Johnson, *Chem. Rev.*, 2016, **116**, 10167.
- T. Yoshikawa and F. You, *Int. J. Mol. Sci.*, 2024, **25**, 3360.
- S. Pandey, M. Karakoti, D. Bhardwaj, G. Tatrari, R. Sharma, L. Pandey, M. J. Lee and N. G. Sahoo, *Nanoscale Adv.*, 2023, **5**, 1492.
- C. Cha, S. R. Shin, N. Annabi, M. R. Dokmeci and A. Khademhosseini, *ACS Nano*, 2013, **7**, 2891.
- M. S. Ahmad, H. He and Y. Nishina, *Org. Lett.*, 2019, **21**, 8164.
- N. Morimoto, K. Morioku, H. Suzuki, Y. Nakai and Y. Nishina, *Chem. Commun.*, 2017, **53**, 7226.
- Y. Matsuki, N. Ohnishi, Y. Kakeno, S. Takemoto, T. Ishii, K. Nagao and H. Ohmiya, *Nat. Commun.*, 2021, **12**, 3848.
- W. Shi, S. Yang, H. Sun, J. Wang, X. Lin, F. Guo and J. Shi, *J. Mater. Sci.*, 2021, **56**, 2226.
- M. Muttaqin, T. Nakamura, Y. Nishina and S. Sato, *J. Mater. Sci.*, 2017, **52**, 749.
- L. J. Konwar, P. M. Arvela and J. P. Mikkola, *Chem. Rev.*, 2019, **119**, 11576.
- Z. Li, L. Jin and C. Cai, *Org. Chem. Front.*, 2017, **4**, 2039.
- Y. Zhang, W. Schilling, D. Riemer and S. Das, *Nat. Protoc.*, 2020, **15**, 822.
- J. Bai, S. Yan, Z. Zhang, Z. Guo and C. Y. Zhou, *Org. Lett.*, 2021, **23**, 4843.
- M. R. Ahmed, Y. K. Cheng and Y. Nishina, *Ind. Eng. Chem. Res.*, 2024, **63**, 7475.
- S. Cailotto, M. Negrato, S. Daniele, R. Luque, M. Selva, E. Amadio and A. Perosa, *Green Chem.*, 2020, **22**, 1145.
- Y. Nishina and S. Eigler, *Nanoscale*, 2020, **12**, 12731.
- H. He, S. Liu, Y. Liu, L. Zhou, H. Wen, R. Shen, H. Zhang, X. Guo, J. Jiang and B. Li, *Green Chem.*, 2023, **25**, 9501.
- P. Chettri, A. Tripathi and A. Tiwari, *Mat. Res. Bull.*, 2022, **150**, 111752.
- M. Alimohammadian and B. Sohrabi, *Nat. Res.*, 2020, **10**, 21325.
- M. Hada, K. Miyata, S. Ohmura, Y. Arashida, K. Ichiyanaagi, I. Katayama, T. Suzuki, W. Chen, S. Mizote, T. Sawa, T. Yokoya, T. Seki, J. Matsuo, T. Tokunaga, C. Itoh, K. Tsuruta, R. Fukaya, S. Nozawa, S. Adachi, J. Takeda, K. Onda, S. Koshihara, Y. Hayashi and Y. Nishina, *ACS Nano*, 2019, **13**, 10103.
- M. R. Ahmed and Y. Nishina, *Bull. Chem. Soc. Jpn.*, 2023, **96**, 568.
- S. Chakraborty, S. Saha, V. R. Dhanak, K. Biswas, M. Barbezat, G. P. Terrasi and A. K. Chakraborty, *RSC Adv.*, 2016, **6**, 67916.
- N. A. Carvajal, D. A. A. Guzman, V. M. Laguna, M. H. Farias, L. A. P. Rey, E. A. Morales, V. A. G. Ramirez, V. A. Basiuk and E. V. Basiuk, *RSC Adv.*, 2018, **8**, 15253.
- C. Su, M. Acik, K. Takai, J. Lu, S. J. Hao, Y. Zheng, P. Wu, Q. Bao, T. Enoki, Y. J. Chabal and K. P. Loh, *Nat. Commun.*, 2012, **3**, 1298.
- J. Zhang, Y. Yang, J. Fang, G. J. Deng and H. Gong, *Chem. – Asian J.*, 2017, **12**, 2524.
- N. Morimoto, Y. Takeuchi and Y. Nishina, *Chem. Lett.*, 2016, **45**, 21.

